Journal of Magnetic Resonance **138,** 225–231 (1999)
Article ID jmre.1999.1732, available online at http://www.idealibrary.com on IDEAL®

A Near-Resonance Solution to the Bloch Equations and Its Application to RF Pulse Design

Zhihua Xu and Andrew K. Chan

Department of Electrical Engineering, Texas A&M University, College Station, Texas 77843-3128

Received August 26, 1998; revised February 8, 1999

A near-resonance expansion of the solution to the Bloch equations in the presence of a radiofrequency (RF) pulse is presented in this paper. The first-order approximation explicitly demonstrates the nonlinear nature of the Bloch equations and precisely relates the excitation profile with the RF pulse when the flip angle is less than $\pi/2$. As an application of this solution, we present a procedure for designing RF pulses to generate symmetric excitation profiles with arbitrary shapes for new encoding approaches such as wavelet encoding. © 1999 Academic Press

Key Words: **Bloch equations; RF pulse design; wavelet-encoding.**

1. INTRODUCTION

Magnetic resonance imaging (MRI) is a powerful tool for obtaining spatially localized information from nuclear magnetic resonance (NMR) of atoms within a sample. The conventional Fourier transform approach to MRI contains three steps: slice-selective excitation, phase encoding, and frequency encoding (*1*). Recently, many new encoding approaches have been developed and implemented as alternatives to phase encoding. New encoding bases have also been found and used to replace the Fourier basis in phase encoding. These bases include nonexclusively wavelets (*2–6*), wavelet packets (*5, 6*), windowed Fourier bases (*7, 8*), a local cosine basis (*9*), and bases derived from the Matching Pursuit (MP) algorithm (*10*). These new encoding approaches have many advantages over the conventional Fourier approach. Higher imaging speed, suppression of motion artifacts, and capability for dynamic imaging are a few examples. In these approaches, transverse excitation profiles are generated by RF pulses along a magnetic field gradient and shaped like the chosen encoding basis functions. This requires the design of linear phase or self-refocusing RF pulses for a few specially shaped excitation profiles with the maximum rotation angle equal to $\pi/2$ so that the highest signal-to-noise ratio (SNR) may be achieved.

In order to design an RF pulse for a specific application, it is necessary to understand the relationship between the excitation profile and the pulse shape. This relationship can be obtained from an analytical solution to the Bloch equations—the phenomenological description of an MRI system. A variety of design algorithms and computer optimization techniques have been proposed in recent years. Warren and Silver's paper (*11*) provides a review of earlier work. References (*12, 13*) give a list of latest results. However, these design algorithms are targeted for specific profile shapes such as rectangular. They are not suitable for RF pulse design to generate arbitrarily shaped excitation profiles. For example, the Shinnar–Le Roux (SLR) algorithm (*14*) transforms the pulse design problem to the design of linear-phase finite impulse response digital filters (FIR), which are bandpass filters for rectangular excitation profiles. Unfortunately, designs of such FIR with arbitrary frequency spectrum are extremely complicated and no specific method is available for the general case (*15*). The inverse scattering algorithm (*12, 16*) requires that the desired magnetization response be specified as a rational polynomial, i.e., as the ratio of two polynomials. This is straightforward for well-known responses such as a selective $\pi/2$ pulse, an inversion pulse, or a π refocusing pulse. However, many desired responses cannot be expressed as rational polynomials. Pulse design through computer optimization typically involves specifying a trial pulse shape and then adjusting the parameters until the response fits the target profile as closely as possible. Though effective, computer optimization is nonintuitive and lacks efficiency. Moreover, it is unlikely to be suitable for the general RF pulse design problem (*11*).

In this paper, a new perturbative expansion of the Bloch equations is proposed that gives exact results for on-resonance. The first-order approximation explicitly demonstrates the nonlinear nature of the Bloch equations. We then utilize this solution to design RF pulses with flip angles up to 75°. The design procedure is very simple and straightforward. Simulations of RF pulses for linear and cubic spline functions have been carried out. The result shows that these linear-phase RF pulses generate excitation profiles very close to the desired ones. In addition, it also provides a very efficient and simple way to obtain an accurate solution of the Bloch equations, which may be used as a forward calculation method for computer optimization approaches to pulse design.

1090-7807/99 $30.00

2. SOLUTION OF THE BLOCH EQUATIONS

In the rotating frame turning at frequency ω_0 about the direction of B_0, the main static magnetic field, we write the Bloch equations (*1*) as

$$\frac{dM_x(\mathbf{r}, t)}{dt} = -\frac{M_x(\mathbf{r}, t)}{T_2} + \Delta\omega M_y(\mathbf{r}, t) \quad [1]$$

$$\frac{dM_y(\mathbf{r}, t)}{dt} = -\frac{M_y(\mathbf{r}, t)}{T_2} - \Delta\omega M_x(\mathbf{r}, t) + \Omega_{1x}(t) M_z(\mathbf{r}, t) \quad [2]$$

$$\frac{dM_z(\mathbf{r}, t)}{dt} = -\frac{M_z(\mathbf{r}, t) - M_z^0(\mathbf{r})}{T_1} - \Omega_{1x}(t) M_y(\mathbf{r}, t), \quad [3]$$

where $\Delta\omega = \gamma\mathbf{G}(t) \cdot (\mathbf{r} - \mathbf{r}_0)$ is the resonance offset and $\Omega_{1x}(t) = \gamma B_1(t)$ is determined by the RF field $B_1(t)$ applied in the x-direction. $\mathbf{r}_0$ is the center of the excitation and $\mathbf{G}(t)$ is the linear magnetic field gradient. $M_z^0(\mathbf{r})$ is the equilibrium value of $M_z(\mathbf{r}, t)$ giving the initial conditions: $M_x(\mathbf{r}, 0) = M_y(\mathbf{r}, 0) = 0$ and $M_z(\mathbf{r}, 0) = M_z^0(\mathbf{r})$. With $\Omega_{1x}(t)$ and $\Delta\omega$ being time-varying, the Bloch equations cannot be conveniently solved in closed form.

In a usual case, the pulse length, τ_p, is much shorter than T_1 and T_2, and we may neglect the relaxation effects. In reality, this assumption is assured in most MRI systems (*17*). An expansion of the solution to the Bloch equations is developed under this assumption. Let

$$M_{xy} = M_x(\mathbf{r}, t) + iM_y(\mathbf{r}, t) \quad [4]$$

$$M_{zy} = M_z(\mathbf{r}, t) + iM_y(\mathbf{r}, t), \quad [5]$$

where $i = \sqrt{-1}$. The Bloch equations are combined to produce two complex equations:

$$\frac{dM_{xy}}{dt} = -i\Delta\omega M_{xy} + i\Omega_{1x}(t)\mathrm{Re}\{M_{zy}\} \quad [6]$$

$$\frac{dM_{zy}}{dt} = i\Omega_{1x}(t) M_{zy} - i\Delta\omega\mathrm{Re}\{M_{xy}\}. \quad [7]$$

When $\Delta\omega = 0$, i.e., on-resonance, these two equations can be easily solved with the given initial conditions. The solution shows that $\mathrm{Re}\{M_{xy}\} = 0$, i.e., $M_x = 0$. When $\Delta\omega \neq 0$, an expansion of the magnetization can be achieved. This may be called a near-resonance expansion. It gives accurate results over a resonance offset range centered at $\Delta\omega = 0$. On the opposite end, Hoult's expansion (*18*) is based on low RF field approximation and thus gives accurate results when $\Delta\omega$ is far away from resonance. Let

$$M_{xy} = M_{xy}^{(0)} + M_{xy}^{(1)} + M_{xy}^{(2)} + \cdots \quad [8]$$

$$M_{zy} = M_{zy}^{(0)} + M_{zy}^{(2)} + M_{zy}^{(2)} + \cdots. \quad [9]$$

After substituting these into Eqs. [6] and [7], we obtain a set of equations of various orders:

$$\frac{dM_{xy}^{(n)}}{dt} = -i\Delta\omega M_{xy}^{(n)} + i\Omega_{1x}(t)\mathrm{Re}\{M_{zy}^{(n)}\}, \quad \text{for all } n \geq 0 \quad [10]$$

$$\frac{dM_{zy}^{(n)}}{dt} = i\Omega_{1x}(t) M_{zy}^{(n)} - i\Delta\omega\mathrm{Re}\{M_{xy}^{(n-1)}\}, \quad \text{for all } n \geq 1 \quad [11]$$

$$\frac{dM_{zy}^{(0)}}{dt} = i\Omega_{1x}(t) M_{zy}^{(0)}. \quad [12]$$

With the initial conditions $M_{zy}^{(0)}(\mathbf{r}, 0) = M_z^0(\mathbf{r})$, $M_{zy}^{(n)}(\mathbf{r}, 0) = 0$ for all $n \geq 1$, and $M_{xy}^{(n)}(\mathbf{r}, 0) = 0$ for all $n \geq 0$, an iterative solution for any $t \in [0, \tau_p]$ is given by

$$M_{zy}^{(0)} = M_z^0(\mathbf{r}) e^{i\alpha(t)} \quad [13]$$

$$M_{xy}^{(n)} = e^{-i\theta(t)} \int_0^t i\Omega_{1x}(\tau)\mathrm{Re}\{M_{zy}^{(n)}(\tau)\} e^{i\theta(\tau)} d\tau, \quad \text{for all } n \geq 0 \quad [14]$$

$$M_{zy}^{(n)} = e^{i\alpha(t)} \int_0^t -i\Delta\omega(\tau)\mathrm{Re}\{M_{xy}^{(n-1)}(\tau)\} e^{-i\alpha(\tau)} d\tau, \quad \text{for all } n \geq 1, \quad [15]$$

where $\theta(t) = \int_0^t \Delta\omega(\tau) d\tau$ and $\alpha(t) = \int_0^t \Omega_{1x}(\tau) d\tau$ are rotation angles caused by the magnetic field gradient and the RF pulse, respectively. When $\Delta\omega = 0$, $M_{xy}^{(n)} = M_{zy}^{(n)} = 0$, for all $n \geq 1$. Thus, $M_{zy} = M_{zy}^{(0)} = M_z^0(\mathbf{r}) e^{i\alpha(t)}$ and $M_{xy} = M_{xy}^{(0)} = iM_z^0(\mathbf{r})\sin(\alpha(t))$, which are exact solutions for on-resonance.

This iterative solution may be viewed as an expansion of magnetization to the resonance offset, $\Delta\omega$. Because the solutions incorporate the effect of $\Delta\omega$ in high order power and exponential terms, this expansion converges very fast. As shown in Fig. 1, only the first two orders are needed to give accurate results for a 90° rectangular pulse in the resonance offset range $[-2\pi, 2\pi]$. For pulses with greater flip angles, higher order expansions are required to give accurate results. Figures 2 and 3 show the results for a 180° truncated sinc pulse with only one sidelobe on both sides. A fifth-order expansion is shown for the longitudinal component of the magnetization, M_z, and a fourth-order one for the transverse components, M_x and M_y. Though higher-order expansion requires more computation, it generally leads to accurate results for a much wider resonance offset range. In this example, it is at least wider than

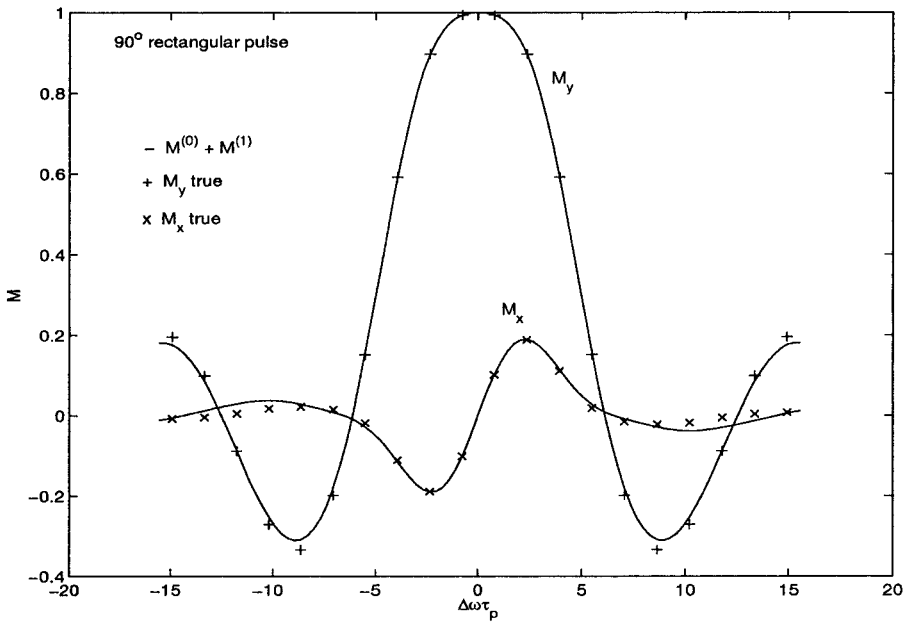

FIG. 1. Computation of M_x and M_y for a 90° rectangular pulse.

$[-5\pi, 5\pi]$. These figures clearly demonstrate that our near-resonance expansion converges over the range centered at $\Delta\omega = 0$. Compared to Hoult's expansion, it shows several advantages. First, it converges faster. Hoult's expansion requires a third-order expansion for a 90° rectangular pulse to achieve the same accuracy. Second, it converges over the range centered at on-resonance, which is a more interesting case. Our near-resonance expansion and Hoult's expansion compliment each other since they have different convergence ranges. Lastly, the first-order approximation in our case is nonlinear, while Hoult's leads to the well-known linear response theory. When applied to RF pulse design, this nonlinear approximation improves the accuracy greatly over the linear response theory (*11*). This will be shown in the next section. Warren's expansion of the effective Hamiltonian converges much faster and gives reasonably good, though in some cases not very accurate,

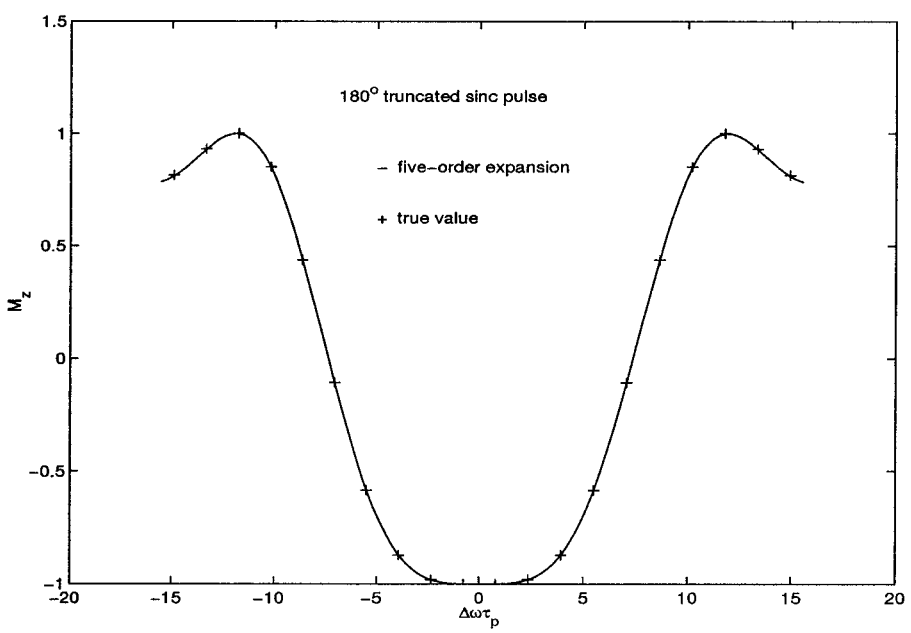

FIG. 2. Computation of M_z for a 180° sinc pulse.

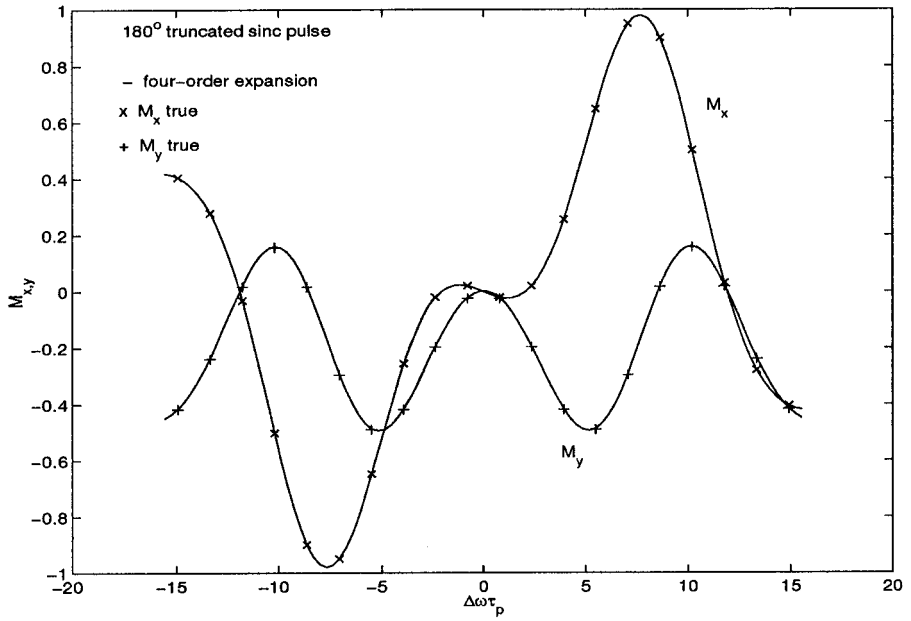

FIG. 3. Computation of M_x and M_y for a 180° sinc pulse.

results with only the first two orders. However, the effective Hamiltonian cannot be applied to RF pulse design.

Of special interest is the first-order approximation for the transverse components of the magnetization, M_{xy}. This expression will be used later for RF pulse design:

$$M_{xy}^{(0)} = iM_z^0(\mathbf{r})e^{-i\theta(t)}\int_0^t \Omega_{1x}(\tau)\cos\,\alpha(\tau)e^{i\theta(\tau)}d\tau. \quad [16]$$

When the magnetic field gradient is constant, at the end of the refocusing magnetic field gradient lobe (*1*), the transverse magnetization is expressed as

$$M_{xy}^{(0)}\left(\mathbf{r}, \frac{3}{2}\tau_p\right) = iM_z^0(\mathbf{r})\int_{-\tau_p/2}^{\tau_p/2}\Omega'_{1x}\left(\tau + \frac{\tau_p}{2}\right)e^{i\Delta\omega\tau}d\tau \quad [17]$$

$$\Omega'_{1x}(t) = \Omega_{1x}(t)\cos\int_0^t \Omega_{1x}(\tau)d\tau. \quad [18]$$

This means that the transverse magnetization is proportional to the Fourier transform of $\Omega'_{1x}(t)$. When the RF field is very low, $\Omega'_{1x}(t) \rightarrow \Omega_{1x}(t)$ and thus Eq. [17] becomes the linear response theory. Therefore, the first-order approximation may also be viewed as a nonlinear generalization of the linear response theory.

3. RF PULSE DESIGN

Given a transverse excitation profile, the design task is to find an appropriately shaped RF pulse to be generated along with a constant magnetic field gradient. From Eq. [17] we see that the function $\Omega'_{1x}(t)$ is related to the excitation profile at the end of the refocusing magnetic field gradient lobe by the inverse Fourier transform. If symmetry around $t = \tau_p$ is assumed, $\Omega'_{1x}(t)$ can be explicitly expressed as

$$\Omega'_{1x}\left(t + \frac{\tau_p}{2}\right) = \frac{1}{2\pi}\int_{-1/2\gamma Gd}^{1/2\gamma Gd}\frac{M_{xy}\left(\mathbf{r}, \frac{3}{2}\tau_p\right)}{iM_z^0(\mathbf{r})}e^{-i\Delta\omega t}d\Delta\omega, \quad [19]$$

where $G = |\mathbf{G}|$ and d is the width of excitation profile along the magnetic field gradient. Since $\Omega'_{1x}(t)$ is a real function and $M_z^0(\mathbf{r})$ is usually assumed uniform, it is required that $M_{xy}(\mathbf{r}, \frac{3}{2}\tau_p)$ be a pure imaginary and symmetric function. For a rectangular excitation profile $\Omega'_{1x}(t)$ is shaped as a sinc function. We see that the design task is to calculate $\Omega_{1x}(t)$ from $\Omega'_{1x}(t)$ using Eq. [18]. It can be rewritten as

$$\Omega_{1x}(t) = \frac{\Omega'_{1x}(t)}{\cos\left[\int_0^t \Omega_{1x}(\tau)d\tau\right]}. \quad [20]$$

This is a complicated integral equation. Fortunately, we need only a numerical solution and a recursive method (*19*) is sufficient for this purpose. The recursive relations are

$$\Omega_{1x}^{(0)}(t) = \Omega'_{1x}(t), \quad [21]$$

$$\Omega_{1x}^{(n+1)}(t) = \frac{\Omega'_{1x}(t)}{\cos\left[\int_0^t \Omega_{1x}^{(n)}(\tau)d\tau\right]}, \quad [22]$$

$$\Omega_{1x}(t) = \Omega_{1x}^{(N)}(t). \quad [23]$$

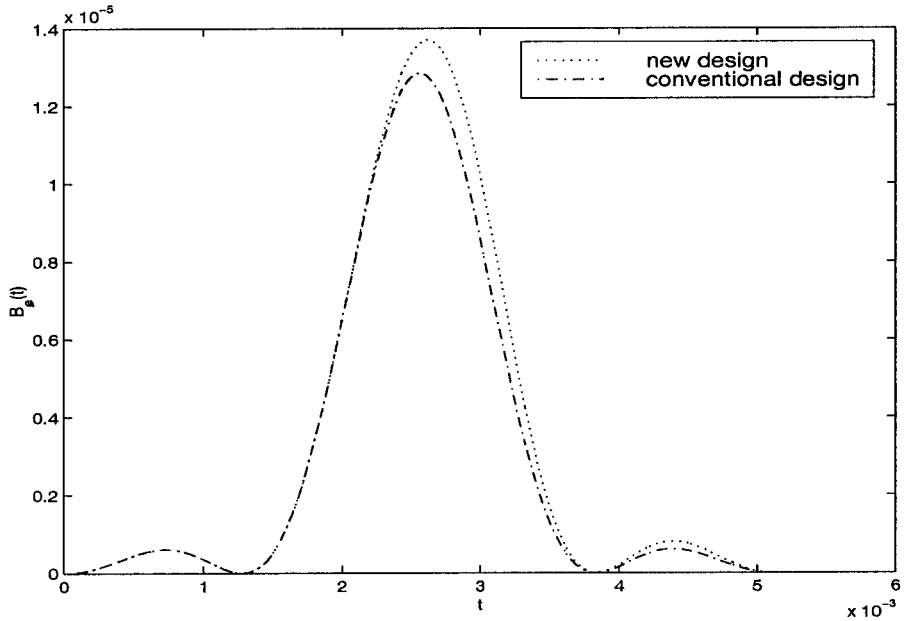

FIG. 4. RF pulses for linear spline.

Although this iterative approach may not converge in all cases, our numerical simulation shows that it converges for flip angles up to 75°. For the design of a 90° RF pulse, this convergence problem can be overcome by scaling a 75° pulse with a similar shape. Since sin(90°) is only slightly larger than sin(75°), we can obtain the 90° RF pulse without losing accuracy.

As examples, we now design the RF pulses for linear spline and cubic spline functions (*20*), which are used to generate the semiorthogonal wavelets (Figs. 4 and 5). The splines and their associated wavelets are chosen as two sets of encoding basis functions when we implement wavelet-encoded MRI in our laboratory. The linear spline function is shrunk by 0.7 so that the flip angles of both pulses are close to 45°. The pulse length, τ_p, is set to be 0.005120 s.

The RF pulses from our design show a big difference in the second half of the pulses. This is because within the first half of excitation the rotation angle $\alpha(t)$ is close to 0, and thus $\cos(\alpha(t))$ is approximately equal to 1. Simulations of pulse

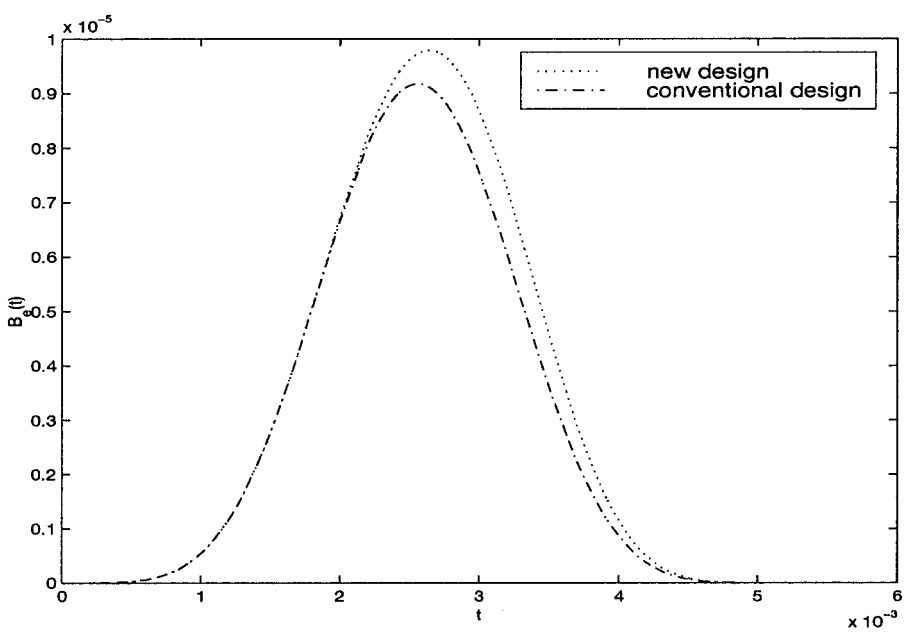

FIG. 5. RF pulses for cubic spline.

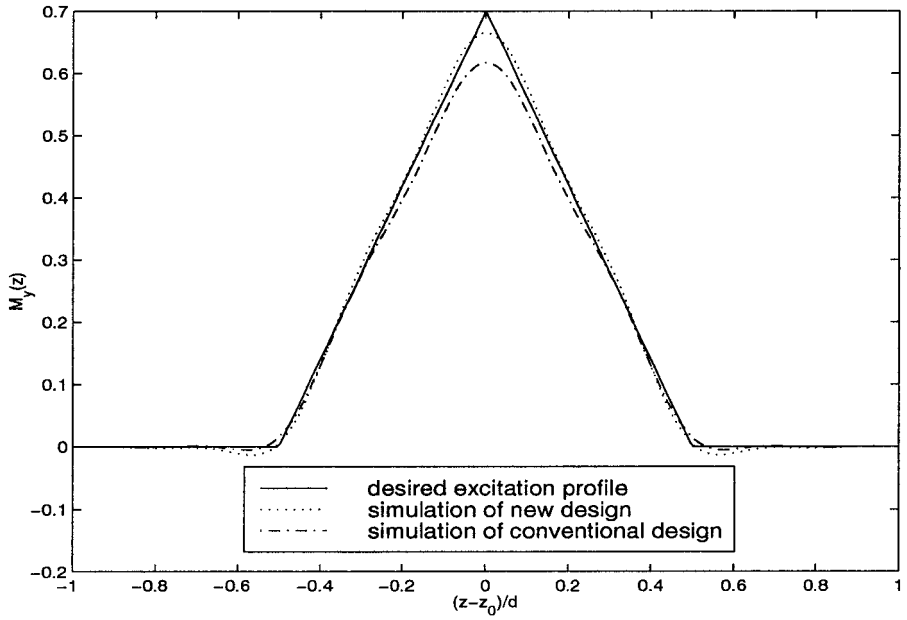

FIG. 6. Simulation for linear spline.

shapes from the conventional design based on the linear response theory and our new design are compared in Fig. 6 and Fig. 7, respectively, for linear spline and cubic spline functions. Apparently, the pulses from the new design excite magnetization profiles much closer to the desired ones. Since the excitation profile is very close to desired function, the perfect reconstruction relationship (*20*) between the function and its dual is kept well when the function is replaced by the excitation profile. This greatly increases the signal-to-noise of the MRI images.

4. CONCLUSION

We have derived a near-resonance expansion of the magnetization that is valid for a much larger range of flip angles and exact for on-resonance. Numerical simulations have been carried out and results agree with prediction very well. The first-order approximation clearly demonstrates the nonlinearity of the Bloch equations and relates the transverse excitation profile to $\Omega'_{1x}(t)$, which is an integral function of $\Omega_{1x}(t)$. The linear response theory is a special case of this first-order

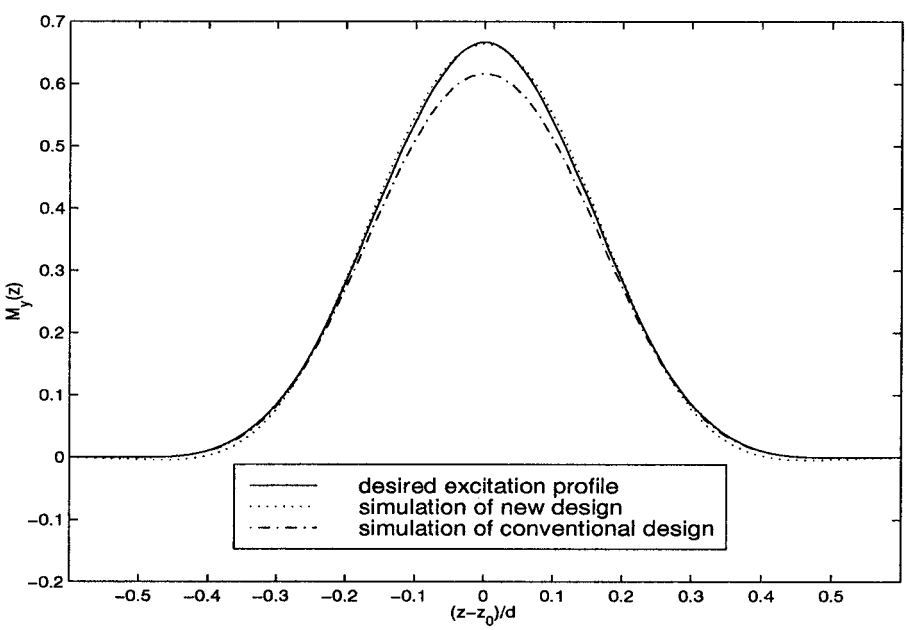

FIG. 7. Simulation for cubic spline.

approximation when $\Omega'_{1x}(t) \rightarrow \Omega_{1x}(t)$. Using this new approximation, generic RF pulses can be designed with much greater accuracy. RF pulse designs for linear and cubic splines have also been carried out.

ACKNOWLEDGMENT

This research project is partially supported by the Texas Higher Education Coordinating Board Grant ARP 999903-168.

REFERENCES

1. M. T. Vlaardingerbroek and J. A. den Boer, "Magnetic Resonance Imaging," Springer-Verlag, Berlin (1996).
2. J. B. Weaver, Yansun Xu, D. M. Healy, and J. R. Driscoll, Wavelet encoded MR imaging, *Magn. Reson. Med.* **24,** 275–287 (1992).
3. L. P. Panych, P. D. Jakab, and F. A. Jolesz, An implementation of wavelet encoded magnetic resonance imaging, *J. Magn. Reson. Imaging* **3,** 649–655 (1993).
4. L. P. Panych and F. A. Jolesz, A dynamically adaptive imaging algorithm for wavelet-encoded MRI, *Magn. Reson. Med.* **32,** 738–748 (1994).
5. J. B. Weaver and D. M. Healy, Signal-to-noise ratios and effective repetition times for wavelet encoding and encoding with wavelet packet bases, *J. Magn. Reson. A* **113,** 1–10 (1995).
6. D. M. Healy and J. B. Weaver, Adapted wavelet techniques for encoding magnetic resonance images, *in* "Wavelets in Medicine and Biology" (A. Aldroubi and M. Unser, Eds.), pp. 297–352, CRC Press, Boca Raton, FL (1996).
7. Y. M. Kadah and Xiaoping Hu, Pseudo-Fourier imaging (PFI): A technique for spatial encoding in MRI, *IEEE Trans. Med. Imaging* **16,** 893–902 (1997).
8. Y. M. Ro and C. H. Oh, Local motion suppression in magnetic resonance imaging, *in* "Medical Imaging 1998: Physics of Medical Imaging" (J. T. Dobbins and J. M. Boone, Eds.), pp. 133–140, SPIE, San Diego (1998).
9. G. Hossein-Zadeh and H. Soltanian-Zadeh, DCT acquisition and reconstruction of MRI, *in* "Medical Imaging 1998: Image Processing" (K. M. Hanson, Ed.), pp. 394–407, SPIE, San Diego (1998).
10. Y. M. Ro, R. Neff, and A. Zakhor, Matching pursuit-ed data acquisition in magnetic resonance imaging, *in* "Medical Imaging 1997: Physics of Medical Imaging" (R. L. Van Metter and J. Beutel, Eds.), pp. 530–540, SPIE, San Jose, CA (1997).
11. W. S. Warren and M. S. Silver, The art of pulse crafting, *in* "Advances in Magnetic Resonance," Vol. 12, pp. 247–388, Academic Press, New York (1988).
12. M. H. Buonncore, "Pulse design using the inverse scattering transform, *Magn. Reson. Med.* **29,** 470–477 (1993).
13. D. E. Rourke, M. J. W. Prior, P. G. Morris, and J. A. B. Lohman, Stereographic projection method of exactly calculating selective pulses, *J. Magn. Reson. A* **107,** 203–214 (1994).
14. J. Pauly, P. Le Roux, D. Nishimura, and A. Macovski, Parameter relations for the Shinnar–Le Roux selective excitation pulse design algorithm, *IEEE Trans. Med. Imaging* **10,** 53–65 (1991).
15. J. G. Proakis and D. G. Manolakis, "Digital Signal Processing: Principles, Algorithms, and Applications," 2nd ed., Prentice-Hall, Englewood Cliffs, NJ (1996).
16. A. E. Yagle, Inversion of the Bloch transform in magnetic resonance imaging using asymmetric two-component inverse scattering, *Inverse Problems* **6,** 131–151 (1990).
17. N. A. Matwiyoff, "Magnetic Resonance Workbook," p. 72, Raven Press, New York (1990).
18. D. I. Hoult, The solution of the Bloch equations in the presence of a varying B1 field—an approach to selective pulse analysis, *J. Magn. Reson.* **35,** 69–86 (1979).
19. E. T. Whittaker and G. N. Watson, "A Course of Modern Analysis," 4th ed., Cambridge University Press, Cambridge, UK (1967).
20. C. K. Chui, "An Introduction to Wavelets," Academic Press, Boston (1992).